signal attenuation constat α in cm^{-1}. More precisely, $\tau(z)/\tau(0) = e^{-\alpha z}$.

[22]This domain is then equivalent to the interior of a square of side π, centered at the origin, in the θ_1-θ_2 plane.

[23]It is well known that single pulses with an area $\theta(0) < \pi$ do not exhibit SIT; see Ref. 1.

[24]Thus, the limits on θ_1 and θ_2 given above can be equivalently expressed as $\theta_1 \leq -\pi$ and $\theta_2 \geq 1.5$.

[25]The $\tau(z)/\tau(0)$ curve (a) in Fig. 5 is artificially depressed for $z \geq 100$ cm, since the calculation of $\tau(z)$ is truncated at $\mu = 100$, and part of the pulse waveform obviously extended beyond that point. See Fig. 6(iii).

[26]Since $|\theta_1| = |\theta_2|$ in the following discussion, we define $|\theta_1| = |\theta_2| \equiv \theta$.

[27]The medium is assumed to be nondegenerate.

[28]Frederic A. Hopf (unpublished).

[29]This has been observed for π pulses in amplifiers and for 0π and 2π pulses in attenuators.

PHYSICAL REVIEW A VOLUME 3, NUMBER 2 FEBRUARY 1971

Light-Scattering Measurement of Concentration Fluctuations in Phenol-Water near its Critical Point*

P. N. Pusey† and W. I. Goldburg
Physics Department, University of Pittsburgh, Pittsburgh, Pennsylvania 15213
(Received 24 August 1970)

The intensity and spectral width of light scattered by a critical mixture of phenol and water have been measured as a function of temperature both above and below the critical temperature T_c. The temperature dependence of the scattered intensity was fitted to $I \propto (T - T_c)^{-\gamma}$ for $T > T_c$ and $I \propto (T_c - T)^{-\gamma'}$ for $T < T_c$. Also measured was the ratio $R_I \equiv I(\Delta T)/I(-\Delta T)$ of intensities scattered at a given temperature interval ΔT above and below T_c. The measured values of γ, γ', and R_I were quite close to the predictions of the 3-D lattice gas model. The spectral width Γ was measured using a photon correlation method, and the data were fitted to $\Gamma = DK^2(1 + K^2\xi_\Gamma^2)$, with the diffusion constant $D = D_0|T - T_c|^{\gamma^*}$ and $\xi_\Gamma = \xi_{0\Gamma}|T - T_c|^{-\nu\Gamma}$ The Fixman term $K^2\xi_\Gamma^2$ (K being the photon momentum transfer) was observed only above the critical temperature. The value of ν and the values of γ^* both above and below T_c were in fairly good agreement with the theory of Kadanoff and Swift. The spectral width measurements also provided the ratio $R_D \equiv D(-\Delta T)/D(\Delta T)$, a quantity for which no theoretical prediction exists. Comparison of this work on phenol-water with that of Swinney and Cummins and others on CO_2 near its gas-liquid critical point reveals remarkable similarities between the two systems.

I. INTRODUCTION

The last few years have witnessed a rapid growth of interest in the critical behavior of systems undergoing a second-order phase transition. Experiments in a wide variety of systems including ferromagnets, simple fluids, and binary liquid mixtures, reveal a striking similarity in their behavior near the critical point. This similarity is a reflection of the fact that fluctuations which develop near the critical point are of sufficiently long range as to be remarkably insensitive to the detailed form of the atomic interactions in the system.[1] As a result, the critical behavior of many of these systems can be characterized by a small number of dimensionless parameters.

The work described here is a study of the temperature dependence of the magnitude and lifetime Γ^{-1} of concentration fluctuations in a critical mixture of phenol and water. Measurements were made both above and below the critical temperature T_c. The lifetime measurements below T_c appear to be the first which have been reported for a binary mixture. A preliminary account of this work has already appeared.[2,3]

The temperature dependence of the magnitude of the fluctuations, which can be characterized by the exponents γ and γ', was measured by following changes in the average intensity I of light scattered by the system. The lifetime of the concentration fluctuations was determined by using a photon correlation method to analyze the fluctuating light intensity. The lifetime is inversely proportional to the mutual diffusion coefficient D whose temperature dependence is described by the exponent γ^*.

In addition to determining γ and γ^*, measurements were made of the following dimensionless intensity and diffusion coefficient ratios:

$$R_I = I(\Delta T)/I(-\Delta T);\quad R_D = D(-\Delta T)/D(\Delta T)\,. \qquad (1)$$

Here the argument $\Delta T(-\Delta T)$ refers to measurements made at equal temperature intervals above (below) T_c. The experimentally determined values of γ and R_I can be compared with predictions of the three-dimensional (3-D) lattice gas model.[4,5] Recent theoretical work of Kadanoff and Swift[6,7]

gives a prediction for the value of γ^*. However, there exists as yet no theoretical prediction for R_D.

Section II of this paper will be devoted to a presentation of the details of the light-scattering measurements. Section III will contain a presentation of the results. These results will be discussed in Sec. IV and compared with theory and with measurements in other systems.

II. EXPERIMENTAL METHODS

A. Sample Preparation

The phenol used in our samples was manufactured by Mallinckrodt.[8] Its major impurities were water and 0.15% hypophosphorous acid (H_3PO_2). The H_3PO_2, which is a preservative introduced to prevent oxidation of the phenol, was removed by repeated washing with distilled water under a nitrogen atmosphere.[9]

The samples were made by diluting the purified phenol-rich solution with distilled water to give the desired concentration. They were judged to have an impurity concentration of $2-3\times10^{-2}$ wt.%, the dominant impurity being H_3PO_2. To remove dust particles, both the phenol-rich solution and the distilled water were filtered with Millipore filters of pore dimension 0.5 μ before being dispensed from a micropipette.[10] The sample tubes were standard Pyrex with an i.d. of 8 mm and a length of about 2 cm. The phenol concentration c of each sample was believed to be known with an absolute accuracy of about 1% and a relative precision of 0.1%.

In an early stage of the work it was observed that phenol-water samples prepared under air exhibited a slow change in phase-separation temperature with time.[11] For example, one of these samples, ostensibly of the critical concentration, showed a change in T_c of 0.15 °C in a two-week period. There seems little doubt that this change in critical temperature was caused by oxidation of the phenol in the solution. Once the H_3PO_2 preservative is removed from phenol, it is therefore necessary to keep oxygen out of the samples in order to prevent this slow time variation of T_c. The residual oxygen was removed by several freeze-pump-thaw cycles after which the sample tubes were sealed *in vacuo*. Samples prepared in this way were found to have phase-separation temperatures which remained constant over a period of several months.

B. Temperature Control

The sample was placed in a constant temperature bath which consisted of a cylindrical glass Dewar containing two quarts of heavy paraffin oil. The sample itself was held in a copper support on the axis of the Dewar. The main heating came from a nichrome-wire heater wound around the outside of the Dewar. This heater was supplied with power sufficient to maintain the bath temperature a few degrees below the desired final temperature. In addition, a nichrome-wire heater coil was placed inside the Dewar. This second heater was wound on a copper cylinder to help establish temperature uniformity. The cylinder was slotted to permit entrance and exit of the light. The inner heater was driven by a temperature controller which has as its sensing element a platinum resistor. By changing the resistance of the Wheatstone bridge to which the platinum resistance thermometer was connected, it was possible to change the bath temperature in steps of 0.013 °C. To minimize temperature fluctuations in the bath, the paraffin oil was stirred.

The performance of the bath was checked with a thermistor temperature sensor connected to a second Wheatstone bridge. The long-term stability of the temperature bath was better than 0.013 °C, and the short-term stability was better than 0.002 °C. The temperature difference across the sample was less than 0.01 °C. With all uncertainties taken into account, temperature was believed to be known to a relative precision of ± 0.01 °C and an absolute accuracy of about 0.1 °C.

C. Light-Scattering Geometry

The light source was a 15-mW He-Ne laser. The scattered light was collected through two circular apertures of diameter $\simeq 0.5$ mm separated by about 2 m. The first aperture was about 10 cm from the sample, and the second was a few centimeters in front of the photomultiplier, an Amperex 56TVP. With this arrangement, roughly one coherence area (A_s) of the photomultiplier is exposed, i.e., the following condition was satisfied[12]:

$$d_1 d_2 n / R\lambda_0 \lesssim 1 , \tag{2}$$

where d_1 and d_2 are the aperture diameters (separated by the distance R), n is the index of refraction of the mixture, and λ_0 is the wavelength of the incident laser beam. When Eq. (2) is satisfied, one is assured that only one spatial Fourier component of concentration fluctuation scatters light into the photodetector. Since each Fourier component scatters light independently in a thermodynamic system, temporal fluctuations in the photocurrent tend to be averaged out if Eq. (2) is not satisfied. Thus nothing is gained in terms of signal-to-noise characteristics for the lifetime measurement by exposing more than one coherence area of the photocathode.

D. Photon Correlation Spectrometer

The lifetime measurements reported in this

paper were made using a photon correlation method to analyze the temporal fluctuations in the scattered light. This method gives a direct measurement of the intensity correlation function $\langle I(t)I(t+\tau)\rangle$, where $I(t)$ is a quantity proportional to the light intensity striking the phototube, and the brackets denote a time or ensemble average.[11] The spectrometer has been described in detail elsewhere, but its principle of operation will be summarized here.[13]

Figure 1(a) shows a typical trace of the time variation of light of fluctuating intensity $I(t)$ falling on a photomultiplier P. The output of P is a series of short pulses, each corresponding to the detection of a single photon, which are fed into a discriminator (D) whose output is shown in Fig. 1(b). The duration of the discriminator pulses was several nanoseconds. The fluctuations in $I(t)$ reflect themselves in a temporal bunching of the discriminator output pulses whose instantaneous rate we define as $C_1(t)$, i.e., $C_1(t) \propto I(t)$. [We will, in fact, take $C_1(t) = I(t)$]. To measure $\langle I(t)I(t+\tau)\rangle$, the correlator performs as follows: One of the pulses from D (occurring at time t, say) initiates a delayed gating pulse of duration τ_g. In order to simplify the algebra, the delay time τ is measured from the time of occurrence of the initiating pulse to the center of the gate pulse, as indicated in Fig. 2. By a circuit arrangement to be described below, any pulse that might occur in the interval τ_g is stored in a counter CTR 2. The first pulse which occurs after the gate interval has ended initiates another gate, and the whole sequence repeats itself for T sec. In these experiments the counting time T was typically of the order of 100 sec. The delay time τ could be varied from ~ 5 μsec to ~ 5 msec, and τ_g was adjusted to be $\frac{1}{5}$ to $\frac{1}{10}$ the maximum delay time used in the measurement. Since the number of counts accumulated in CTR 2 is proportional both to the number $I(t)$ of gates per sec and to

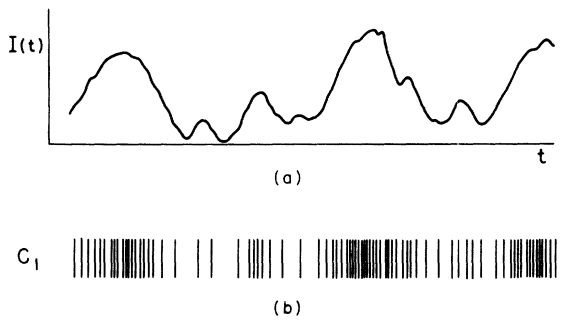

FIG. 1. (a) Fluctuating intensity $I(t)$ falling on photomultiplier tube (P). (b) Photomultiplier pulses after having passed through amplifier-discriminator (D).

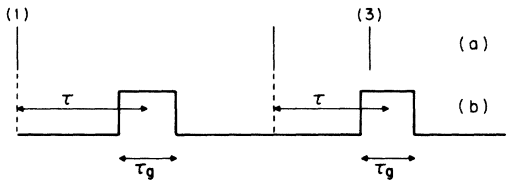

FIG. 2. (a) Expanded view of pulses from discriminator (D). (b) Output of the delayed gate generator (GD). In this figure, pulses (1) and (2) initiate the delayed gates. Pulses (1), (2), and (3) all get counted in CTR 1, whereas only pulse (3) is counted in CTR 2. The situation depicted here corresponds to the scaling factor s equal to unity.

$I(t+\tau)$, the counting rate in the gate interval τ_g, it follows that[14]

$$C_{12} = \int_{\tau'=\tau-(\tau_g/2)}^{\tau'=\tau+(\tau_g/2)} \langle I(t)\, I(t+\tau')\rangle\, d\tau' \,. \tag{3}$$

Here C_{12} is the mean number of coincidence counts accumulated per sec, and it has been assumed that the optical field is stationary.

For thermally induced fluctuations, the light will be Gaussian, for which[15]

$$\langle I(t)I(t+\tau)\rangle = \langle I(t)\rangle^2 + \left|\langle E(t)\, E^*(t+\tau)\rangle\right|^2 , \tag{4}$$

where $\langle E(t)\, E^*(t+\tau)\rangle$ is the electric field autocorrelation function.[12]

Near the critical point in a binary mixture, the fluctuations in electric susceptibility, which scatter the light, are almost entirely due to concentration fluctuations. These fluctuations decay by diffusion. The diffusional decay implies that[16]

$$\left|\langle E(t)E^*(t+\tau)\rangle\right| = \langle\, |E(0)|^2\rangle\, e^{-\Gamma\tau} \,. \tag{5}$$

Combining Eqs. (3)–(5) and inserting a factor β which accounts for the loss of temporal coherence in the photocurrent owing to a small degree of spatial incoherence of the scattered light across the photocathode,[12] one has

$$C_{12} = \langle C_1\rangle^2 \int_{\tau-(\tau_g/2)}^{\tau+(\tau_g/2)} (1+\beta e^{-2\Gamma\tau'})\, d\tau'$$

$$= \langle C_1\rangle^2 \tau_g \left(1+\beta e^{-2\Gamma\tau}\, \frac{\sinh\Gamma\tau_g}{\Gamma\tau_g}\right) \,. \tag{6}$$

In these experiments, the chosen values of d_1, d_2, and R, gave $\beta \simeq 0.9$. The quantity of interest Γ is obtained from the slope of a semilog plot of $(C_{12}/\langle C_1\rangle^2\tau_g - 1)$ as a function of τ for fixed τ_g. For most measurements, $\sinh(\Gamma\tau_g)/\Gamma\tau_g$ could be taken equal to one.

As described so far, the photon correlation spectrometer has a serious deficiency, viz., it can only be used at counting rates $\langle C_1\rangle$ sufficiently low that

the probability of a pulse occurring in the time interval τ is very small. This is because the instrument is "dead" during this delay time, so that pulses occurring then cannot initiate a subsequent gate.[17] The result is a distortion of the measured correlation by loss of counts in CTR 2. Were it possible to produce the delay τ by a continuous delay line of one sort or another, this difficulty would not arise. Unfortunately, satisfactory delay lines with a delay time in the range of interest have not been readily available.[18] To circumvent this difficulty to some degree, one can artificially reduce the number of gate-initiating pulses without reducing the number of counts which are recorded during the gating intervals. This was done in the following manner: Pulses from the discriminator D are divided into two channels. The pulses in channel 1 go directly to one input of a coincidence circuit (CC) as indicated in Fig. 3. The counting rate C_1 is monitored by the counter CTR 1. The pulses in channel 2, however, pass through a scaler (S) which gives one output pulse for every s input pulses. Typically $s = 10$. The output of S initiates a delayed gate (DG) as previously described. The scaling factor s is selected to assure that the probability of two pulses from S occurring in the interval τ is small.

Scaling the pulses in channel 2 obviously alters their time distribution; the probability of a gate being initiated at time t is no longer solely dependent on $I(t)$ but depends also on the time at which the previous gate was initiated. In fact, the pulses are debunched in the sense that the occurrence of a gate-triggering pulse at a given time sharply decreases the probability of a subsequent pulse occurring a short time later. This is because s-1 pulses must accumulate in the scaler before the second gate-triggering pulse is emitted. Nevertheless, it can be shown that, provided the counting time $T \gg 1/\Gamma$ and the total number of coincidence counts $C_{12}T$ accumulated is large, the sole effect of the scaler on C_{12} is to introduce a factor s in the denominator of Eq. (6),[13] i.e.,

$$C_{12} = \frac{C_1^2 \tau_g}{s} \left(1 + \beta e^{-2\Gamma\tau} \frac{\sinh \Gamma\tau_g}{\Gamma\tau_g} \right) . \qquad (7)$$

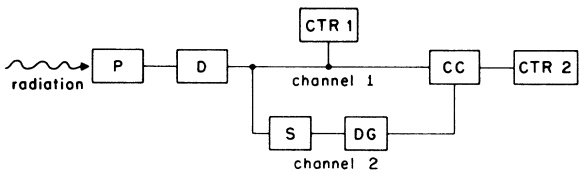

FIG. 3. Simplified block diagram of photon correlation spectrometer. All symbols are defined in the text.

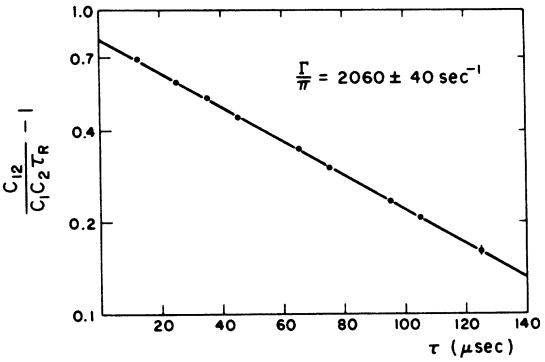

FIG. 4. Typical result of a decay-rate measurement with the photon correlation spectrometer. Except for the one point on the far right, statistical errors were too small to be indicated. Here $C_2 = C_1/S$.

It can also be shown that scaling down the counting rate in channel 2, rather than avoiding loss of counts by reducing the incident light intensity, leads to much higher coincidence counting rates.[13] In part, this large enhancement is due to the debunching effect of scaling mentioned above.

While the values of Γ of interest in these experiments were relatively small (300 sec$^{-1} \lesssim \Gamma \lesssim$ 30 000 sec^{-1}), the instrumentation was capable of measuring very short correlation times down to values of the order of nanoseconds.[14] It should be mentioned that the photon correlation method described here provides the same physical information about the scattered light as the commonly used "self-beat" or homodyne method developed by Ford and Benedek.[2,16,19] A comparison of the two methods has been given elsewhere.[13]

Figure 4 shows a typical set of measurements using the photon correlation spectrometer. In our experiments the photomultiplier dark current was approximately 200 counts/sec, and C_1 was typically $\sim 5 \times 10^3$ counts/sec. Uncorrelated counts such as those due to stray room light or dark current contribute to the first term on the right-hand side of Eq. (7) but not to the second. On inclusion of this noise contribution, one has

$$\frac{sC_{12}}{\langle C_1 \rangle^2 \tau_g} - 1 = \delta \frac{\sinh \Gamma\tau_g}{\Gamma\tau_g} e^{-2\Gamma\tau} , \qquad (8)$$

where $\delta = \beta r^2/\langle C_1 \rangle^2$. The quantity $r/\langle C_1 \rangle$ is the ratio of the counting rate due to the light under study r to the total counting rate $\langle C_1 \rangle$. For the set of measurements shown in Fig. 4, $\delta \simeq 0.8$ and $\beta \simeq 0.9$.

A useful parameter characterizing the signal-to-noise ratio in this type of experiment is $n \equiv \langle C_1 \rangle/\Gamma$, which is the average number of photon counts per correlation time. For the data in Fig. 4, n is approximately equal to 0.8. The ap-

paratus has been successfully used at values of n as small as 0.1. Of course when n is small, the data must be accumulated over longer times (T) if the signal-to-noise ratio is not to suffer. The errors on the points in Fig. 4 correspond to the statistical variation in the total number of counts accumulated in the interval T.[20] Except where indicated, these errors were smaller than the size of the data points.

III. RESULTS

A. Phase Diagram

Determination of the phase diagram was not one of the main aims of this experiment. However, because most of the existent data on the phenol-water system appeared to be several decades old,[21] it was decided to make a rough study of the phase diagram in order to locate the critical point. Accordingly, nine samples were prepared ranging in concentration around the expected critical concentration. The phase-separation temperatures T_P were determined as follows: The sample was allowed to reach equilibrium in the one-phase region. The temperature was then lowered in steps of about 0.013 °C until phase separation was observed. In all cases, this separation occurred unambiguously after one such temperature drop. T_P was then taken to be midway between the temperatures prior and subsequent to the temperature step causing separation. The relative precision of the measurement was thus about ± 0.007 °C.

Theory predicts that the coexistence curve is characterized by the equation[1,4]

$$|c - c_c| \propto (T_c - T_p)^{\beta}, \tag{9}$$

where c_c is the critical concentration. For the 3-D lattice gas model, $\beta \simeq 0.31$. Experimental investigations of various critical systems usually give values of β in the range $0.30 < \beta < 0.36$.[1,4] With this in mind, the sample concentration was plotted against $(T_c - T_p)^{1/3}$, and the results are shown in Fig. 5. T_c was taken to be the phase-separation temperature of the sample at c =34.0-wt% phenol. It can be seen that the data fit fairly well to two straight lines, but that the lines do not cross the concentration axis at the same point. This could indicate a "flat top" to the phase diagram, as has been found by some other investigators.[22] Flat tops are usually attributed to the effect of impurities. However, in Fig. 5, a plot is also given with $\beta = 0.28$. Again the data fit reasonably well to straight lines. For $\beta = 0.28$ there is no flat top to the phase diagram, and the critical concentration is $c_c = 35.0 \pm 0.5$-wt% phenol.

As an added check on this graphical method of determining c_c, the following experiment was performed: Four samples were prepared with concentration of 34.5-, 35.0-, 35.5- and 36.0-wt% phenol. All four samples had the same measured T_p. According to the lever rule, a sample at the critical concentration should, on cooling to the critical temperature, develop a phase boundary dividing it into equal volumes of each phase. This occurred most nearly in the sample for which c = 35.0-wt% phenol. The critical temperature was found to be $T_c = 65.50 \pm 0.01$ °C with an absolute accuracy of about 0.1 °C.[23]

B. Intensity Measurements

The intensity measurements reported here were performed by Bak in our laboratory.[24] Measurements of the scattered light intensity were made at two scattering angles, $\theta = 30.4 \pm 0.5°$ and $74.8 \pm 0.5°$. Experiments were carried out above the critical temperature and in both the low-density (water-rich) and high-density (phenol-rich) phases below T_c. The results will be compared with the Ornstein-Zernike prediction[25,26]

$$I_c \propto k_B T \left(\frac{\partial \mu}{\partial c}\right)_T^{-1} (1 + K^2 \xi^2)^{-1}, \tag{10}$$

where I_c is the intensity of scattered light due to concentration fluctuations, k_B is Boltzmann's constant, μ is an appropriately defined chemical potential difference,[16] ξ is the correlation length, and K is the photon momentum transfer, i.e.,

$$K = (4\pi n/\lambda_0) \sin\tfrac{1}{2}\theta . \tag{11}$$

The quantity $(\partial \mu/\partial c)_T$ determines the magnitude of the concentration fluctuations, and the length ξ is a measure of the spatial range of correlation between fluctuations at different points. The temper-

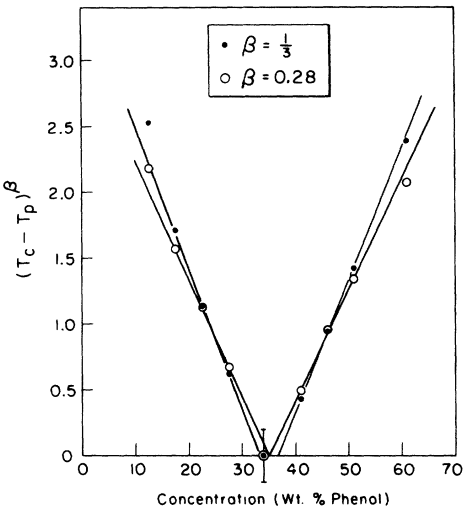

FIG. 5. Phase diagram of the phenol-water system in the vicinity of the critical concentration.

ature dependences of these quantities are characterized, respectively, by γ and ν for $T > T_c$,[27] i.e.,

$$\left(\frac{\partial \mu}{\partial c}\right)_T \propto (T - T_c)^{\gamma} , \tag{12}$$

$$\xi^{-1} \propto (T - T_c)^{\nu} . \tag{13}$$

Below the critical temperature the behavior is characterized by the exponents γ' and ν'.

In these experiments, the factor $K^2\xi^2$ in Eq. (10) was much less than unity, whence one expects that

$$T/I_c \propto (T - T_c)^{\gamma} . \tag{14}$$

The light-scattering geometry was identical to that described in Sec. II C except that the photomultiplier aperture diameter was enlarged to 1.2 mm. [Since the spatial-coherence condition, Eq. (2), need not be satisfied for the intensity measurements, there is no reason not to use a larger aperture.] The intensity of the laser beam transmitted through the sample was monitored with an E.G. and G SGD-100 photodiode. The values of I_c were corrected for variations in the source light intensity. After a suitable warmup time (about 1 h), these variations were generally less than 5%.

The measurements at $\theta = 30.4°$ are shown in Fig. 6. According to Eq. (14), the exponents γ and γ' are obtained from the slopes of this log-log plot of T/I_c as a function of $|T - T_c| \equiv |\Delta T|$. The straight lines A, B, and C in Fig. 6 are, respectively, least-squares fits to the data for $T > T_c$, $T < T_c$ (high-density phase), and $T < T_c$ (low-density phase). The data points on lines A and B designated by crosses were taken at exactly the same optical geometry. The same is true of the measurements denoted by open circles on lines A and C. The solid circles on line A represent a different run in which the scattering angle was reset as accurately as possible to 30.4°.

A word should be said concerning the method of measuring I_c. The total amount of light (I_{tot}) reaching the photomultiplier at a given scattering angle arises from three sources. These are scattering from concentration fluctuations, density fluctuations, and spurious scattering from the sample tube. To obtain an estimate of these latter two contributions, separate measurements were made using samples cells which contained pure water and pure phenol. To a first approximation, an appropriately weighted averaged of the light intensities from these two samples should provide a measure of the background, i.e.,

$$I_c \simeq I_{tot} - c_c I_{phenol} - (1 - c_c) I_{water} .$$

Here, I_{phenol} and I_{water} denote the light scattered by the pure components. The method of background correction which we have described fails to take into account the fact that the pure phenol and pure water samples have a different optical match to the sample cell than does the critical phenol-water mixture. However, since the total background was only 7% of I_{tot} at even the smallest values of I_c, the correction procedure was regarded as satisfactory.

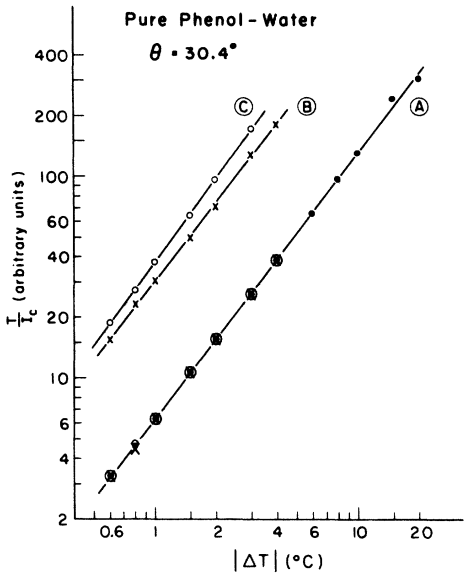

FIG. 6. Temperature dependence of the reciprocal light intensity at scattering angle $\theta = 30.4°$. Curves A, B, and C, respectively, correspond to $T > T_c$, $T < T_c$ (high-density phase), and $T < T_c$ (low-density phase).

Finally, there remains the problem of multiple scattering. To minimize its effects, the measurements were not carried very close to the critical temperature. At the smallest value of $(T - T_c)$ shown in Fig. 6, the incident beam attenuation was 15%. At $(T - T_c) = 1.5$ °C, multiple scattering was negligible. By normalizing $I_c(T)$ to the transmitted beam intensity as described above, correction was automatically made for attenuation of the incident and singly scattered beams. However, no correction was attempted to account for multiply scattered light reaching the phototube. It should be noted that discarding the data points in Fig. 6 for $|T - T_c| < 1.6$ °C would not affect seriously the conclusions drawn from the data.

The data in Fig. 6 yield the critical exponents γ and γ' and the ratios R_I shown in Table I. The fact that the points in this figure fall on a straight line confirms the earlier statement that the factor $K^2\xi^2$ is much less than unity. This observation was further corroborated by similar measurements carried out above T_c at $\theta = 74.8°$. Even at this large scattering angle, $\ln(T/I_c)$ was proportional to $\ln(T - T_c)$ over the temperature interval 0.6 C° $< T - T_c <$ 20 C°. In addition, the value of γ obtained from this plot agreed with that obtained at the smaller scattering angle.

C. Decay Rate Measurements

In a binary mixture, the inverse lifetime Γ of the concentration fluctuations is expected to be given by the equation[28,29]

$$\Gamma = DK^2(1+\xi_\Gamma^2 K^2) , \tag{15}$$

when $K\xi_\Gamma \lesssim 1$. In the above equation, D is the binary diffusion coefficient and ξ_Γ is a correlation range. This range is not necessarily expected to have the same value as its counterpart ξ obtained from intensity measurements.[30] Following Chu,[31] we define the exponent ν_Γ by the equation

$$\xi_\Gamma = \xi_{0\Gamma}(T-T_c)^{-\nu_\Gamma} . \tag{16}$$

According to the fluctuation dissipation theorem, the diffusion constant D in (15) can be written as the product of two factors, one of which is the thermodynamic derivative $(\partial\mu/\partial c)_T$ and the other being the time integral of a flux correlation function,[32] i.e.,

$$D = \alpha^*\left(\frac{\partial\mu}{\partial c}\right)_T \propto \left(\frac{\partial\mu}{\partial c}\right)_T \int_0^\infty \langle J_c(t)J_c(t+\tau)\rangle\, d\tau, \tag{17}$$

where J_c is the flux of the component of concentration c. The temperature dependence of D is described by the critical exponent γ^*, i.e.,

$$D \propto |T-T_c|^{\gamma^*} . \tag{18}$$

Since I_c^{-1} is also proportional to $(\partial\mu/\partial c)_T$, from measurements of both I_c and the decay rate Γ, one may determine the exponent which characterizes the critical behavior of the dynamic factor α^* alone. The temperature dependence of this variable will be discussed in Sec. IV A.

Measurements of the temperature variation of Γ in phenol-water were made at the critical concentration c_c. The following angles and temperature intervals were studied:

(a) $T > T_c$, $\theta = 33.0 \pm 0.5°$, $0.1 \lesssim (T-T_c) \lesssim 12$ C° ;

(b) $T > T_c$, $\theta = 145.2 \pm 0.5°$, $0.1 \lesssim (T-T_c) \lesssim 2$ C° ;

(c) $T < T_c$, high-density phase (phenol-rich),

$\theta = 33.0°$, $0.1 \lesssim (T_c - T) \lesssim 6$ C° ;

(d) $T < T_c$, low-density phase (sater-rich), $\theta = 33.0°$, $0.1 \lesssim (T_c - T) \lesssim 3$ C° .

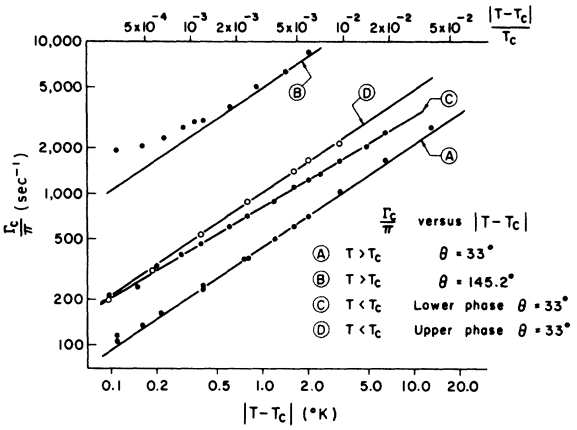

FIG. 7. Temperature dependence of the decay rate Γ at two scattering angles, both above and below the critical temperature.

The maximum value of $|T-T_c|$ was limited by the available intensity of the scattered light. The results are shown in Fig. 7, where $\log_{10}(\Gamma_c/\pi)$ is plotted against $\log_{10}|T-T_c|$. The corrected decay rate Γ_c in this graph takes into account the weak concentration dependence of the index of refraction in the two-phase region. This correction, which is made to refer all data to the same value of K, is

$$\Gamma_c = n_0^2\,\Gamma_{\text{measured}}/n^2 ,$$

where n_0 is the refractive index of the critical mixture above T_c. To a sufficiently good approximation, $n^2 = \phi_1 n_1^2 + (1-\phi_1)n_2^2$.[33] The indices n_1 and n_2 refer to the pure phenol and pure water, and ϕ_1 denotes the volume fraction of phenol in the phase in question. The ratio n_0^2/n^2 varied by less than 10% over the temperature range covered.

The upward curvature at small $(T-T_c)$ in curves

TABLE I. Comparison of critical exponents and ratios measured in this work with similar measurements in two simple fluids.

	$T>T_c$		$T<T_c$ Low-density phase					$T<T_c$ High-density phase				
	γ	γ^*	γ'	γ^*	R_D	R_I	R_I/R_D	γ'	γ^*	R_D	R_I	R_I/Rd
Phenol-water	1.32 (0.03)	0.68 (0.03)	1.36 (0.03)	0.68 (0.03)	2.29 (0.13)	5.6 (0.3)	2.4 (0.4)	1.28 (0.04)	0.60 (0.02)	1.84 (0.09)	5.0 (0.3)	2.7 (0.3)
CO_2	1.26 (0.1)	0.73 (0.02)	1.1 (0.4)	0.66 (0.05)	1.99 (0.23)	4.4 (?)	2.21 (>0.30)		0.72 (0.05)	1.93 (0.19)	4.4 (?)	2.28 (>0.25)
SF_6		1.26 (0.02)		0.632 (0.002)					0.635 (0.003)			

A and B is attributed to the Fixman ($\xi_\Gamma^2 K^2$) term in Eq. (15). The data shown in Fig. 7 were analyzed as follows: From the curves A and B, a rough value of ξ_Γ was extracted. This value of ξ_Γ was used in conjunction with Eq. (15) to obtain DK^2 for $\theta = 33.0°$. Then a computer least-squares fit to the data for DK^2 at $\theta = 33.0°$ was made to the equation

$$DK^2_{33.0} = D_0 K^2_{33.0}(T - T_c)^{\gamma^*} .$$

It can be seen that the three high-temperature points on curve A fall slightly off the straight line formed by the other points. It is not known whether this is a real effect or an experimental error. In the least-squares analysis, therefore, two fits were made, one to all the data and the other to the data excluding the three high-temperature points. The first gave

$$DK^2_{33.0}/\pi = (451 \pm 4)\,(T - T_c)^{0.695 \pm 0.007}\ \text{sec}^{-1} , \quad (19)$$

and the second gave

$$DK^2_{33.0}/\pi = (441 \pm 4)\,(T - T_c)^{0.672 \pm 0.007}\ \text{sec}^{-1} . \quad (20)$$

Finally, a three-parameter fit, with T_c floating, was made to the data excluding the three high-temperature points, to check for possible error in the measurement of T_c. This yielded

$$DK^2_{33.0}/\pi = (440 \pm 5) \times [(T - T_c) + (0.002 \pm 0.01)]^{0.675 \pm 0.02}\ \text{sec}^{-1} , \quad (21)$$

i.e., the measured value of T_c lies within the error of the calculated value. Combining the results of these three analyses, the data are certainly in agreement with

$$DK^2_{33.0}/\pi = (445 \pm 10)\,(T - T_c)^{0.68 \pm 0.03}\ \text{sec}^{-1} . \quad (22)$$

The line in curve A is

$$\Gamma_c/\pi = 445(T - T_c)^{0.68}\ \text{sec}^{-1} .$$

The data of curve B were analyzed using Eqs. (15), (16), and (22) to obtain the magnitude and approximate temperature dependence of ξ_Γ. This analysis gave the result

$$\xi_\Gamma = (86 \pm 10)\,(T - T_c)^{-\nu_\Gamma}\ \text{Å},$$

with $\nu_\Gamma = 0.58 \pm 0.1$.

The measurements at $\theta = 33.0°$, $T < T_c$ (curves C and D) give no evidence of upward curvature at small $T_c - T$ although a small Fixman correction can be noted at $\theta = 33.0°$, $T > T_c$ (curve A). This result is not unexpected on theoretical grounds since the correlation length ξ is expected to be smaller for $T < T_c$ than for $T > T_c$. For instance, classical theories predict $\xi(\Delta T)/\xi(-\Delta T) = \sqrt{2}$.[1,34] If this value of the ratio is appropriate for phenol-water, the Fixman correction in Eq. (15) would cause, in this experiment, an immeasurably small effect on curves C and D.

Since the Fixman term is negligible below T_c, the temperature dependence of Γ_c is contained entirely in the first term of Eq. (15). Analysis of the data gives the following results: High-density phase (phenol-rich, curve C):

$$\Gamma_c/\pi = (820 \pm 20)\,(T_c - T)^{0.60 \pm 0.02}\ \text{sec}^{-1}; \quad (23)$$

low-density phase (water-rich, curve D):

$$\Gamma_c/\pi = (1020 \pm 30)\,(T_c - T)^{0.68 \pm 0.03}\ \text{sec}^{-1} . \quad (24)$$

The values of γ^* are displayed in Table I. Also shown are the ratios R_D defined in Eq. (1). These ratios, which are obtained directly from Eqs. (22), (23), and (24), are of physical interest only to the degree to which they are independent of $|\Delta T|$, i.e., if γ^* has the same value above and below T_c. Since this was not exactly the case, it must be stated that the ratios in Table I were evaluated at $|\Delta T| = 1\,°\text{C}$.

D. Further Experimental Considerations

(*a*) *Equilibration times.* When the temperature of the sample is changed, one must, of course, wait for it to come to equilibrium at the new temperature. For $T > T_c$, only heat transport is involved in this equilibration process, and it was found necessary to wait less than 1 h between measurements at different temperatures. For $T < T_c$, the equilibration process after a change of temperature involves mass transport across the phase boundary as well as heat transport. It was found that for phenol-water this process took as much as 8 or 10 h to complete. This meant that a maximum of two data points could be taken per day, and collection of data for $T < T_c$ was therefore tedious. To check that this waiting period was long enough, the points for $T < T_c$ at $T_c - T = 2.0\,°\text{C}$ were taken after a four-day wait. It can be seen that these points lie well on curves C and D of Fig. 7.

When taking data below T_c the temperature was always decreased, since in this case the mass transport involved in the equilibration process was aided rather than hindered by gravity.

(*b*) *Heating of the sample by the laser.* The possibility that the laser beam might be causing an appreciable rise in temperature in the sample was checked by monitoring the scattered-light counting rate immediately after unblocking the laser beam. A decreasing counting rate was interpreted as indicating heating, causing a decrease in the light-scattering cross section of the mixture. Such heating was found for $(T - T_c) \lesssim 0.5\,°\text{C}$, where the cross section is large enough that an appreciable fraction of the incident light is scattered. When heating was observed, the laser beam was attenuated by an appropriate amount with filters.

(c) *Effect of multiple scattering on spectral width measurements.* It has been observed by several authors that, while multiple scattering is difficult to correct for in intensity measurements, it does not appear seriously to affect spectral width measurements. Recently, Volochine and Berge[35] have performed experiments which confirm that the measured value of Γ is independent of sample cell size even when multiple scattering is present. They give the following explanation for this result[36]: Multiply scattered light arriving at the photodetector generally originates from a larger volume in the sample than does singly scattered light. This means that in most cases the coherence area for multiple scattering can be expected to be considerably smaller than the coherence area A_s for singly scattered light. The result is that if one uses a photodetector with aperture $\simeq A_s$, as is usually the case, the exposed photocathode area will contain many multiple-scattering coherence areas. Thus the photoelectrons arising from multiply scattered light will be virtually uncorrelated in time and, as with stray light, they will contribute only to the first term of Eq. (8). Multiple scattering, therefore, has no effect on the measurement of Γ other than reducing the signal-to-noise ratio. Nevertheless, we note that, in our experiment, multiple scattering was negligible over most of the temperature interval covered. To be precise, at $T - T_c = 0.1C°$, the attenuation length of the incident beam was about 1 cm, which was roughly the sample tube diameter.

(d) *Effect of impurities.* It has been noted in Sec. II A that the dominant impurity in the sample was H_3PO_2 and that its estimated concentration was $2-3\times10^{-2}$ wt%. To determine the effect of this impurity on the critical exponents and ratios, an additional set of experiments was performed on a phenol-water sample containing 5.7 wt% of H_3PO_2. Though the results of this study have been reported elsewhere,[37] we summarize them here. The impurity produced a large drop in the critical temperature (~30 °C) and a slight change in the critical concentration of the phenol and water components. It did not, however, change appreciably either the critical exponents or R_D. Only the parameter R_I was different in this highly impure system. The greatest change was in the high-density phase value of R_I below T_c. Here

$$R_I(\text{impure}) = 3.8 \pm 0.4,$$

as compared with $R_I = 5.0 \pm 0.3$ in the pure system. It thus appears that impurities in small amounts do not appreciably alter the critical parameters in this system.

IV. DISCUSSION

A. Critical Exponents

While the exponents γ and γ^* have been measured in a number of one- and two-component fluids above the critical temperature, there exist very few measurements in the two-phase region.[38] Our intensity measurements below T_c lead to values of γ' (Table I) which are in good agreement with the prediction of the 3-D lattice gas model, namely, $\gamma' = 1.31 \pm 0.05$.[4] The value of γ, while in reasonable agreement with the observations of others, is slightly but significantly different from the 3-D lattice gas value $\gamma = 1.25 \pm 0.003$.

It has previously been noted that a measurement of Γ near T_c provided a rough estimate of the important critical exponent ν, which describes the temperature dependence of the correlation length ξ_Γ. The value we obtain ($\nu = 0.58 \pm 0.1$) is not inconsistent with either the classical value, $\nu = 0.5$ or the 3-D lattice gas value $\nu = 0.64$.[4]

We turn now to a discussion of the exponent γ^*. The theory of Swift[7] predicts that the diffusion coefficient D should be given by $D = D_0 |T - T_c|^\nu$. Thus, the values of γ^* appearing in Table I should be compared with the theoretical values of ν and ν'. It may be seen that they are in much better agreement with the nonclassical values $\nu \simeq 0.64$, $\nu' \simeq 0.67$ than with classical values $\nu = \nu' = 0.5$.[4]

Our values for γ^* can also be compared with the results of similar experiments on other systems. For $T > T_c$, eight or ten such experiments have now been performed, measuring either D in a liquid mixture or the analogous thermal diffusivity χ_T in a pure fluid.[3,7] To our knowledge, only three of these experiments include extensive measurements in the two-phase region. These are the present experiment, the work of Swinney and Cummins[39] on CO_2, and the measurements of Benedek[16,19] on SF_6. With the exception of $\gamma^* = 1.26$ for SF_6 above T_c, for which no theoretical explanation has yet been given, all the experimental values of γ^* lie in the range $0.60 < \gamma < 0.75$.

It was noted in Sec. III C that D is the product of a thermodynamic variable $(\partial\mu/\partial c)_T$ and a dynamic variable α^* and that by measuring both I_c and Γ, the temperature dependence of α^* can be determined. According to Eqs. (12), (17), and (18),

$$\alpha^* = D \Big/ \left(\frac{\partial\mu}{\partial c}\right)_T \propto (T - T_c)^{-\psi}, \tag{25}$$

where $\psi = \gamma - \gamma^*$. In a one-component fluid, the analogs of D, $(\partial\mu/\partial c)_T$, and α^* are, respectively, the thermal diffusivity, the inverse isothermal compressibility κ_T^{-1}, and the thermal conductivity Λ. From the data of Table I, it may be seen that $\psi = 0.64 \pm 0.04$ and $\psi' = 0.68 \pm 0.04$. For many years it was expected that α^* and Λ should at most show a weak divergence near the critical point.[6,7] More recently, stronger divergences have been predicted: Based on a classical van der Waal's model,

Fixman obtained $\psi = \psi' = 0.5$.[40] The nonclassical calculations of Kadanoff and Swift lead to $\psi = \psi' \simeq 0.67$.[6,7] Our values of ψ are clearly in better agreement with the results of Kadanoff and Swift.

We conclude this section by drawing attention to the slightly different temperature dependences of both D and $(\partial\mu/\partial c)_T$ in the two-phase region. All current theories of critical phenomena predict symmetrical behavior in the two-phase region.[1] However, it is possible that the observed dissymmetry is due to concentration-dependent effects, which would vanish on close enough approach to the critical temperature. For example, when $T < T_c$, we might assume that

$$D^H = D_0(T_c - T)^{\gamma^*}[1 + \delta c_H(T)],$$

$$D^L = D_0(T_c - T)^{\gamma^*}[1 + \delta c_L(T)].$$

Here D^H and D^L are the measured diffusion coefficients on the high- and low-concentration sides of the critical concentration. The term $\delta c_H(T)$ and $\delta c_L(T)$ are regarded as temperature-dependent corrections to the "true" diffusion coefficient $D_0(T_c - T)^{\gamma^*}$, and we therefore expect

$$\delta c_H(T_c) = \delta c_L(T_c) = 0.$$

In the immediate neighborhood of the critical point, it seems reasonable to assume $\delta c_H(T) = -\delta c_L(T)$, whence

$$\tfrac{1}{2}(D^H + D^L) = D_0(T_c - T)^{\gamma^*}.$$

It is interesting to note that if this average is performed on the data of curves C and D of Fig. 7, the results can be fitted to:

$$(\Gamma_c/\pi) = (920 \pm 25)(T_c - T)^{0.64 \pm 0.03}\ \text{sec}^{-1}.$$

This value of γ^* includes our value of $\gamma^* = 0.68 \pm 0.03$ for $T > T_c$ in its experimental error.

A similar dissymmetry between phases was observed in the spectral-width measurements in CO_2.[39]

B. Ratios

Possibly the most interesting result of this experiment appears in a comparison of our measurements of the ratios R_I, R_D, and R_I/R_D with the work of others. These quantities, defined in Eq. (1), may be expressed in terms of dynamic and thermodynamic variables as shown in Table II. All of the variables in Table II have already been defined, and the relations which appear there follow from Eqs. (10), (15), and (17), assuming $K\xi$, $K\xi_\Gamma \ll 1$.

TABLE II. Expressions for the ratios R_I and R_D in one- and two-component systems.

System	R_I	R_D	R_I/R_D
Two component	$\left(\frac{\partial\mu}{\partial c}\right)_{\Delta T} \Big/ \left(\frac{\partial\mu}{\partial c}\right)_{\Delta T}$	$\frac{D(-\Delta T)}{D(\Delta T)}$	$\frac{\alpha^*(\Delta T)}{\alpha^*(-\Delta T)}$
One component	$\frac{\kappa_T^{-1}(-\Delta T)}{\kappa_T(\Delta T)}$	$\frac{\chi_T(-\Delta T)}{\chi_T(\Delta T)}$	$\frac{\Lambda(\Delta T)}{\Lambda(-\Delta T)}$

We first discuss the intensity ratio R_I. In both phenol-water and CO_2 this number is of the order of 4 or 5[2,41] and has the same value in both phases. Values of R_I around 4 have also been obtained for He,[4] and Xe,[41] and methanol-cyclohexane.[42,43] Classical theories give $R_I = 2$, whereas the 3-D lattice gas model predicts $R_I = 5.2 \pm 0.5$, the exact theoretical result depending on the lattice used for the calculation. The number quoted here represents an average for simple cubic, fcc, and bcc lattices.[4]

Turning now to R_D, it is seen from Table I that this parameter is approximately 2 in both CO_2 and phenol-water. Perhaps even more interesting is the near equality of R_I/R_D in these two systems. Since this ratio involves only time integrals of correlation functions [see Eq. (17)], it may be more amenable to calculation then the directly measurable quantity R_D. As yet however, there exists no theoretical prediction of either of these quantities. It is obvious that more experimental work must be done to determine if similar results are found in other systems.

ACKNOWLEDGMENT

We are grateful to Dr. C. S. Bak for carrying out the intensity measurements.

*Work supported by the National Science Foundation.

†Present address: IBM, T. J. Watson Research Center, Yorktown Heights, N. Y. 10598.

[1]See, for example, L. P. Kadanoff, W. Gotze, D. Hamblen, R. Hecht, E. A. S. Lewis, V. V. Palciauskas, M. M. Rayl, J. Swift, D. Aspnes, and J. Kane, Rev. Mod. Phys. 39, 395 (1967).

[2]P. N. Pusey and W. I. Goldburg, Phys. Rev. Letters 23, 67 (1969).

[3]For a recent review containing an extremely comprehensive bibliography, see B. Chu, Ann. Rev. Phys. Chem. 21, 145 (1970).

[4]See, for example, the review article by M. E. Fisher, *Reports on Progress in Physics* (The Physical Society of London, England, 1967), Vol. 30, Part 2, p. 615.

[5]R. B. Griffiths, Phys. Rev. 158, 176 (1967).

[6]L. P. Kadanoff and J. Swift, Phys. Rev. 166, 89 (1968).

[7]J. Swift, Phys. Rev. 173, 257 (1968).

[8]Reagent No. 0028, Mallinckrodt Chemical Works, St. Louis, Mo.

[9]In a previous publication (see Ref. 2), the preservative was erroneously stated to be H_3PO_4.

[10]It was found that phenol attacked the regular cellulose

Millipore filters. Accordingly, the solvent-resistant Solvinert filters were used.

[11]P. N. Pusey and W. I. Goldburg, Appl. Phys. Letters 13, 321 (1968).

[12]For a discussion of spatial and temporal coherence, see M. Born and E. Wolf, *Principles of Optics*, 2nd ed. (Macmillan, New York, 1964), Chap. X. See also, L. Mandel and E. Wolf, Rev. Mod. Phys. 37, 231 (1965).

[13]P. N. Pusey, Ph. D. thesis, University of Pittsburgh, 1969 (unpublished).

[14]B. L. Morgan and L. Mandel, Phys. Rev. Letters 16, 1012 (1966). These authors were the first to use a single-channel correlation spectrometer for spectral width measurements.

[15]C. Kittel, *Elementary Statistical Physics* (Wiley, New York, 1958), Sec. 28. See also, Mandel and Wolf, Ref. 12.

[16]See, for example, G. B. Benedek, in *Polarization Matière et Rayonnement, Livre de Jubilé en l'Honneur du Professeur A. Kastler* (Presses Universitaires de France, Paris, 1968).

[17]Actually the deadtime is $\tau_g/2+\tau$.

[18]It should be noted that recent advances in integrated circuit technology have made simple the construction of shift registers having delay times ranging from tenths of microseconds to many seconds. Such a shift register can be used as a quasicontinuous delay line.

[19]N. C. Ford and G. B. Benedek, Phys. Rev. Letters 15, 649 (1965).

[20]We assume here that the standard deviation in the number of counts accumulated in T sec in the counter CTR 2 is $(C_{12}T)^{1/2}$.

[21]*International Critical Tables of Numerical Data, Physics, Chemistry, and Technology*, edited by E. W. Washburn (McGraw-Hill, New York, 1928), Vol. 3.

[22]See, for example, O. K. Rice, J. Phys. Colloid Chem. 54, 1293 (1950).

[23]In a previous publication [C. S. Bak and W. I. Goldburg, Phys. Rev. Letters 23, 1218 (1969)] it was erroneously stated that $T_c = 66.05\,^{\circ}\mathrm{C}$.

[24]C. S. Bak (private communication).

[25]L. D. Landau and E. M. Lifshitz, *Statistical Physics* (Addison-Wesley, Reading, Mass., 1958), Chap. 12.

[26]M. E. Fisher, J. Math. Phys. 5, 944 (1964).

[27]See, for example, Ref. 3.

[28]W. D. Botch and M. J. Fixman, J. Chem. Phys. 42, 199 (1965).

[29]B. U. Felderhof, J. Chem. Phys. 44, 602 (1966).

[30]K. Kawasaki, Phys. Letters 30A, 325 (1969), and to be published; R. A. Ferrell, Phys. Rev. Letters, 24, 1169 (1970). These authors predict $\xi_\Gamma = (\frac{3}{5})^{1/2}\xi$.

[31]B. Chu, N. Kuwahara, and M. Tamsky, J. Chem. 51, 2449 (1969).

[32]S. A. Rice and P. Gray, *The Statistical Mechanics of Simple Liquids* (Interscience, New York, 1965), Sec. 7.3.

[33]C. J. F. Bottcher, *Theory of Electric Polarization*, (Elsevier, New York, 1952).

[34]Here we have assumed following Kawasaki (Ref. 30), that $\xi \propto \xi_\Gamma$.

[35]B. Volochine and P. Bergé, J. Phys. (Paris) 31, 819 (1970).

[36]This explanation was previously advanced by F. T. Arecchi, M. Giglio, and U. Tartari, Phys. Rev. 163, 186 (1967).

[37]See Bak and Goldburg, Ref. 23.

[38]M. Giglio and G. B. Benedek, Phys. Rev. Letters 23, 1145 (1969). Also see Ref. 3 for a complete tabulation of relevant data as of 1969.

[39]H. L. Swinney and H. Z. Cummins, Phys. Rev. 171, 152 (1968).

[40]M. Fixman, J. Chem. Phys. 47, 2808 (1967).

[41]M. Vicentini-Missoni, J. M. Levelt Sengers, and M. S. Green, Phys. Rev. Letters 22, 389 (1969). These authors have extracted values of R_I for a number of one-component systems including He, Xe, and CO_2. In this reference R_I is denoted as Γ.

[42]Y. Balta and C. C. Gravatt, J. Chem. Phys. 48, 3839 (1968).

[43]Another critical mixture in which R_I and R_D have been measured is phenol-water 5.7-wt% H_3PO_2. In that system, these parameters have values close to those reported here. See Ref. 23.

PHYSICAL REVIEW A VOLUME 3, NUMBER 2 FEBRUARY 1971

Fluid-Solid Phase Transition of a Hard-Sphere Bose System

Jean-Pierre Hansen, Dominique Levesque, and Daniel Schiff
*Laboratoires de Physique Theorique et Hautes Energies**
91, *Orsay, France*

The ground-state energy of a system of hard-sphere bosons of diameter σ is calculated by a variational method using a Jastrow wave-function for the fluid phase and a "localized" Jastrow times a Gaussian wave function for the solid phase. The transition densities are $\rho_{\text{fluid}} = 0.23 \pm 0.02$ particles/σ^3 and $\rho_{\text{solid}} = 0.25 \pm 0.02$ particles/σ^3.

A well-known peculiarity of liquid helium at very low temperature is that the density at which it crystallizes is more than twice as small as the crystallization density of the heavier inert gases; the crystallization density of helium-4 (Ref. 1) at 0 °K, expressed in units of particles/σ^3 (where σ is the diameter of the Lennard-Jones 12-6 potential[2]) is 0.425 and that of helium-3 (Ref. 3) is 0.385. On the other hand, the reduced density of, say, argon at the triple point is 0.84. This peculiarity can be accounted for, at least qualitatively, by the large zero-point motion of the helium atoms.